Bioorganic Chemistry 92 (2019) 103272

Contents lists available at ScienceDirect

Bioorganic Chemistry

journal homepage: www.elsevier.com/locate/bioorg

Triazolopyridazine derivatives: Synthesis, cytotoxic evaluation, c-Met kinase activity and molecular docking

Eman M. Ahmed[a], Nadia A. Khalil[a], Azza T. Taher[a,b], Rana H. Refaey[c,*], Yassin M. Nissan[c,d]

[a] Pharmaceutical Organic Chemistry Department, Faculty of Pharmacy, Cairo University, Cairo, Egypt
[b] Pharmaceutical Organic Chemistry Department, Faculty of Pharmacy, October 6 University, Giza, Egypt
[c] Pharmaceutical Chemistry Department, Faculty of Pharmacy, October University for Modern Sciences and Arts (MSA), Giza, Egypt
[d] Pharmaceutical Chemistry Department, Faculty of Pharmacy, Cairo University, Kasr Elini St., Cairo 11562, Egypt

ARTICLE INFO

Keywords:
Triazolopyridazines
Pyridazines
Cytotoxic activity
c-Met kinase

ABSTRACT

Novel series of some triazolo[4,3-*b*]pyridazine derivatives were designed and synthesized. All the newly synthesized compounds were evaluated for their cytotoxic activity at 10^{-5} M concentration towards 60 cancer cell lines according to USA NCI protocol. Most of the synthesized compounds showed good activity against SR (leukemia) cell panel. The most active compounds, **2f** and **4a** were subjected for further evaluation at a five dose level screening and their efficacy for c-Met kinase inhibition was determined *in vitro*. Binding mode of these derivatives was explored *via* molecular docking.

1. Introduction

C-Met kinase is a tyrosine kinase receptor that is activated by binding of hepatocyte growth factor (HGF), resulting in receptor dimerization followed by downstream signalling [1]. In normal cells, this pathway plays a key role in normal embryonic development, as well as damage repair and wound healing in adults [2–6]. It has been reported that the c-Met kinase pathway is deregulated in various human cancers, such as colorectal, lung and gastric and other carcinomas, through the overexpression of the c-Met kinase receptor. This deregulation is associated with tumour proliferation, angiogenesis and metastasis, as well as poor prognosis [7]. In addition, c-Met kinase has also been implicated in tumour resistance to therapy, including EGFR and VEGFR inhibitors such as gefitinib, cetuximab and panitumumab [8]. Therefore, the inhibition of c-Met kinase using small molecules, particularly through the targeting of the ATP-binding site as demonstrated for other kinases, is an attractive strategy for pursuing novel anticancer agents [1,9]. Crizotinib and cabozantinib are c-Met kinase inhibitors that have been recently approved by FDA for treatment of various cancers, along with several other agents, such as tivantinib and fortinib, reported to be undergoing clinical trials [10–14]. Among the compounds reported to show high c-Met kinase inhibitory potency, as well as high selectivity towards c-Met kinase in comparison to other kinases, are triazolopyridazine derivatives, Fig. 1. Hence, this research was centered on the synthesis and investigation of the cytotoxic potential of novel triazolopyridazines. Compounds exhibiting promising results were further evaluated as c-Met kinase inhibitors *in vitro*. Compound **I** showed IC_{50} value of 9.3 nM while that for compound **II** was less than 100 nM and finally compound **III** 3 nM [15–20]. These results encouraged further developments of new pyrazolopyridazines targeting c-Met kinase hoping to discover better inhibitors for this key enzyme.

2. Results and discussion

2.1. Chemistry

The synthetic route for the target compounds **2a-i, 4a,b** and **6a,b** is outlined in Schemes 1 and 2. The intermediates **1a-i** and **3b** were prepared from the commercially available 3,6-dichloropyridazine and the appropriate amines or amides *viz*; anthranilamide or salicylamide as a starting materials, according to previously reported procedure [21,22]. The target triazolopyridazine derivatives **2a-i** and **4a,b** were obtained in 65–84% yield by heating the precursors **1a-i** or **3a,b** with isonicotinic acid hydrazide in n-butanol for 6 h.

Supporting evidence for the structure of the two new key compounds **1f**, **1i** and the final targets **2a-i** was achieved on the basis of elemental analyses and various spectroscopic methods. Spectral data IR, ^{1}H NMR, ^{13}C NMR and MS were found to be in full agreement with the proposed structure. IR spectra of **1f**, **1i** and **2a-i** showed prominent bands of NH str. at 3476–3267 cm^{-1}. In ^{1}H NMR spectra, the aromatic protons were observed at the expected region. The signals due to NH protons (controlled with D_2O) were resonated at δ 9.86–10.39 ppm. In

* Corresponding author.
E-mail address: rhosny@msa.eun.eg (R.H. Refaey).

https://doi.org/10.1016/j.bioorg.2019.103272
Received 22 May 2019; Received in revised form 15 August 2019; Accepted 9 September 2019
Available online 10 September 2019
0045-2068/

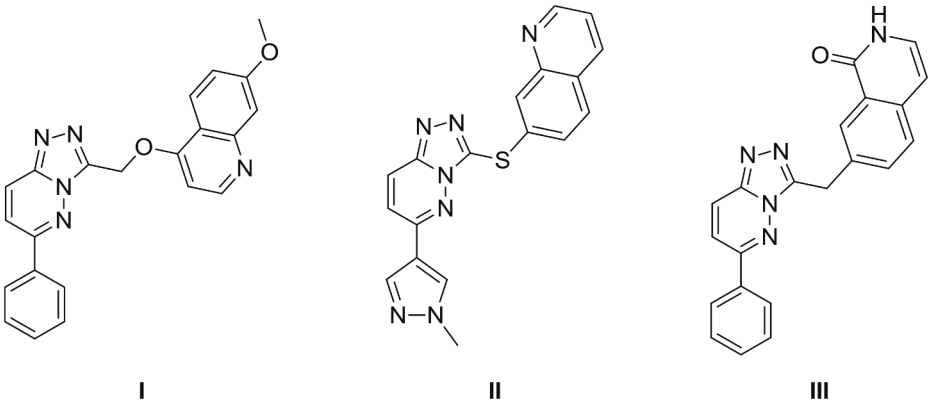

Fig. 1. Structures of lead compounds (I, II, IIII) with known c-Met kinase inhibitory activity.

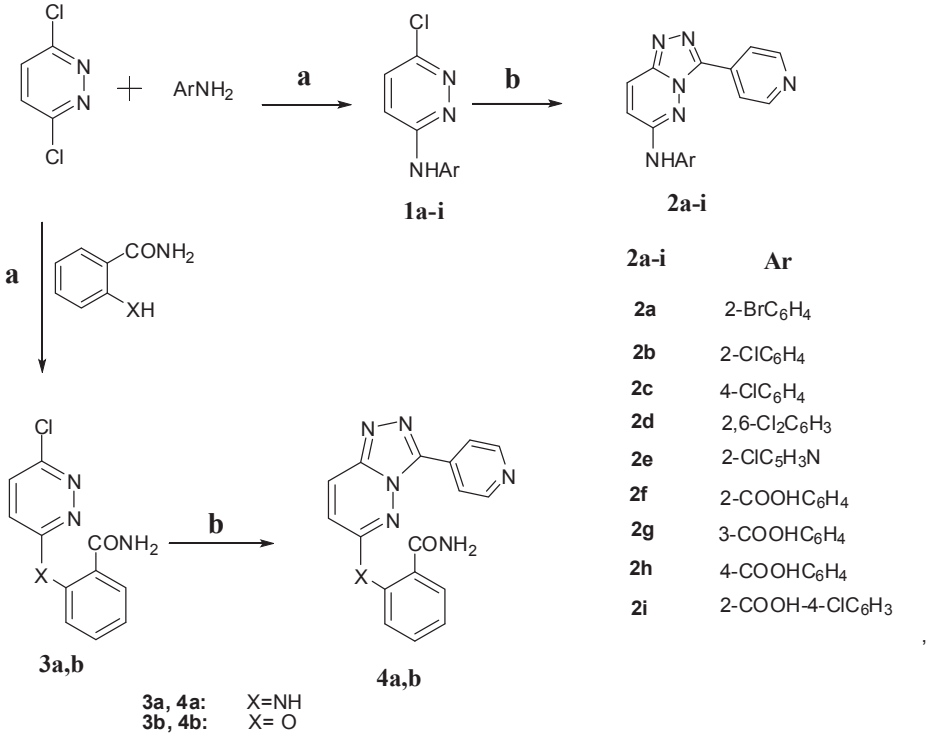

Scheme 1. Regents and condition: (a) isopropanol/k_2CO_3/reflux 4 h. (b) INH/butanol/reflux 6 h.

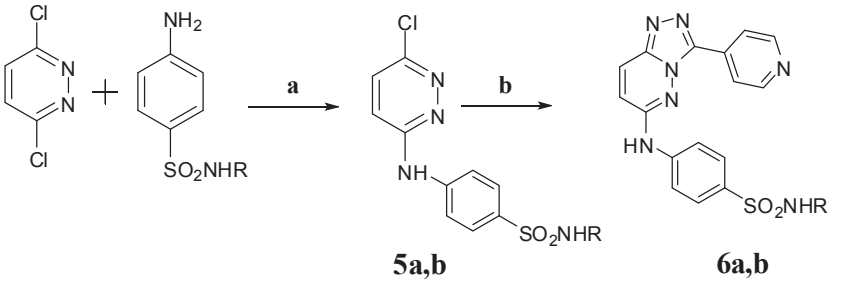

Scheme 2. Reagents and condition: (a) isopropanol/k_2CO_3/reflux 4 h, (b) INH/butanol/reflux 6 h.

Table 1
Percentage growth inhibition (GI%) of *in vitro* sensitive tumour cell lines for compounds **2f** & **4a** at 10^{-5} M.

Compound	Mean growth inhibition %	Range of growth inhibition %	Most sensitive cell panel/cell line growth %
2f	42.18	20–75	L/CCRF-CEM 69, L/MOLT-4 46, L/RPMI- 8226 32, L/SR 75, NSCLc/A549 31, NSCLc/NCI-H460 49, NSCLc/NCI-H522 64, Cc/SW-620 43, Cc/HCT-116 68, Cc/HCT-15 71, Cc/HT29 33, M/LOX IMVI 75, M/SK-MEL-5 43,Oc IGROV1 51, Rc/ACHN 32, Bc/MCF-7 63, Bc/MDA-MB 468 70
4a	45.87	18–89	L/CCRF-CEM 77, L/K-560 35, L/MOLT-4 58, L/RPMI-8226 36, L/SR 78, NSCLc/NCI-H460 60, NSCLc/NCI-H522 81, Cc/HCT-116 71, Cc/HCT-15 72, Cc/HT-29 30, Cc/SW620 50, CNSc/SF-268 41, M/LOX IMV1 89, M/SK-MEL-5 52, Oc/IGROV1 36, Oc/OVCAR-8 30, Rc/ACHN 41, Rc/SN 12C 39, Bc/MCF-7 68, Bc/BT-549 45, Bc/MDA-MB-468 77

L leukemia, *NSCLc* non-small cell lung cancer, Cc colon cancer, *CNSc* CNS cancer, *M* melanoma, *Oc* ovarian cancer, *Rc* renal cancer and *Bc* breast cancer.

Scheme 2, using methodology previously described [22], the intermediates **5a, b** were synthesized from a commercially available 3,6-dichloropyridazine and either sulphanilamide or sulphadiazine. Thereafter, reaction of **5a, b** with isonicotinic acid hydrazide afforded **6a, b** in 76–72% yield.

IR spectra of compounds **6a, b** showed two bands for SO_2 str. in the range of 1315–1323 cm^{-1} and 1134–1153 cm^{-1}. The structures were further established by ^1H NMR spectral data. The additional D_2O exchangeable signals due to SO_2NH_2 protons in **6a** and SO_2NH in **6b** were observed at δ 5.75 and δ 6.65 ppm respectively.

2.2. Biological studies

2.2.1. Cytotoxic activity

All the synthesized compounds underwent preliminary cytotoxic assay against the full panel of 60 cell lines, at a single dose of 10^{-5} M. The preliminary screening results showed compounds **2e**, **2h** and **6b** were completely devoid of cytotoxic activity. It was also reported that compounds **2g**, **4b** and **6a** showed moderate activity only against renal cancer cell lines while compound **2d** only showed cytotoxic activity against leukemia cell lines. On the other hand, compounds **2a, 2b, 2c**, **2f**, **2i** and **4a** exhibited significant cytotoxic activity against a wide variety of cell lines. However, only compounds **2f** and **4a** showed considerable cytotoxic activity with a broad spectrum against several cancer cell lines (Table 1).

Accordingly, compounds **2f** and **4a** were selected for further evaluation at a five-dose assay with concentrations ranging from 0.01 to 100 μM, the response parameters GI_{50}, TGI_{50} and LC_{50} against each cell line were calculated. GI_{50} represents molar concentration of the compound that produce 50% decrease in the net cell growth and is viewed as a growth inhibitory level of effect; TGI (cytostatic activity) is the molar concentration of the compound that results in total growth inhibition; LC_{50} is the cytotoxicity parameter that reflects the molar concentration needed to cause 50% net cell death (Table 2).

Additionally, the mean graph midpoints (MG_MID), representing the average of GI_{50} and TGI over all the cell lines (full panel), as well as subpanel averages for each of the tested molecules were also calculated. Furthermore, a selectivity index was calculated by dividing the full panel MID by their individual subpanel MID and was used to determine the criterion for selectivity of a compound [23] (Tables 3 and 4**).**

Compounds **2f** and **4a** showed effective growth inhibition with MG-MID values of GI_{50} 9.51 and 8.69 μM, respectively and MG-MID values of TGI (MG-MID) of 30.13 and 24.53 μM, respectively. The calculated selectivity index ranged from 0.57 to 1.68 and from 0.30 to 1.65, for compounds **2f** and **4a** respectively. Selectivity index values lower than 3 indicate lack of selectivity [23]. These values suggest that compounds **2f** and **4a** have non-selective, broad spectrum antitumor activity against all tumor subpanels tested.

2.2.2. In vitro c-Met kinase inhibition

In light of the promising cytotoxic activity exhibited by compounds **2f** and **4a**, their activity as c-Met kinase inhibitors *in vitro* was evaluated in an attempt to explain their cytotoxic mechanism of action. The profile of **2f** and **4a** against c-Met kinase was evaluated by employing the standardized assay methodology [24,25]. The results were reported as % activity change compared to control (Table 5). Furthermore, the data was used to plot dose response graph which was used to determine the IC_{50} value for both compounds (Fig. 2).

Upon examination of the results, it was found that both compounds, **2f** and **4a** showed increasing inhibition of c-Met kinase activity with increasing concentrations, with compound **2f** showing higher inhibitory activity than compound **4a**. Compound **2f,** at 100 μM inhibited the c-Met kinase activity by 51% and exhibited an IC_{50} value of 106.9 μM. On the other hand, compound **4a**, at 100 μM concentration inhibited the c-Met kinase activity by 35%, with an IC_{50} value of 242.2 μM (Fig. 2).

2.3. Molecular docking

In order to investigate the molecular basis of the mechanism of action of the synthesized compounds, the interactions formed between the synthesized compounds and the c-Met kinase receptor was explored by carrying out docking studies. The docking studies revealed that the synthesized compounds adopted different orientations into the ATP-binding pocket. The compounds showing high to moderate cytotoxic activity (**2a, 2b, 2c, 2f, 2i & 4a**), adopted “Bent U-shaped” conformations, with different degrees of bending, within the ATP binding site of the c-Met kinase receptor (Fig. 3). This binding mode is reported to be characteristic for compounds type I inhibitors selective to c-Met Kinase [26].

In addition to the distinctive conformation, Type I inhibitors are also reported to form distinctive interactions with the ATP binding site, a hydrogen bonds with Met1160 in the hinge region, as well as π stacking with Tyr1230 residue [10,27]. Upon examination of the selected docked poses of the most active compounds, it was found that the previously mentioned compounds were able to form the π stacking with Tyr1230 residue, whereas only compound **4a** was able to form a hydrogen bond with Met1160 residue backbone NH and the triazole ring (Fig. 4). The difference in the ability to form the hydrogen bond is due to the different orientation the molecules adopt in the binding pocket. The triazolopyridazine ring of compound **4a** is oriented towards the hinge ring thus able to form the hydrogen bond with Met1160 residue, and the phenyl ring is oriented towards the Tyr1230 (Fig. 4, top). For compounds **2f**, the pyridine ring is oriented towards Tyr1230 residue forming the π stacking, therefore the molecule is unable to interact with the Met1160 residue (Fig. 4, middle). The remaining compounds, **2a, 2b, 2c & 2i,** adopted a different conformation, where the triazolopyridazine is oriented towards the Tyr1230 residue, leaving the phenyl ring oriented towards the Met1160 residue, and the compound unable to form hydrogen bond. This orientation is in agreement with the orientation reported by Albrecht et al. and Buchanan et al., where the crystal structures of c-Met kinase co-crystallized with triazolopyridazine derivatives (Fig. 1, compounds I and II) where the triazolopyridazine moiety is responsible for the π stacking [15,20]. Compounds I and II were able to form Hydrogen bonds with Met1160 through

Table 2
In vitro anticancer activity of compounds **2f** and **4a** against 60 human cancer cell lines.

Panel cell line		Compound					
		2f			4a		
		GI_{50}	TGI	LC_{50}	GI_{50}	TGI	LC_{50}
Leukaemia							
	CCRF-CEM	4.28	> 100	> 100	3.12	17.40	> 100
	HL60(TB)	32.5	> 100	> 100	14.30	39.60	> 100
	K-562	15.1	> 100	> 100	11.10	60.40	> 100
	MOLT-4	6.99	> 100	> 100	5.18	30.40	> 100
	RPMI-8226	–	–	> 100	3.43	17.40	> 100
	SR	5.23	> 100	> 100	2.83	14.6	> 100
Non-Small Cell Lung Cancer							
	A549/ATCC	13.30	62.00	> 100	–	–	–
	HOP-62	15.40	33.50	73.10	9.93	22.40	50.30
	HOP-92	16.90	35.80	76.00	–	–	–
	NCI-H226	–	–	–	15.00	44.40	> 100
	NCI-H23	14.10	54.20	> 100	15.00	40.40	> 100
	NCI-H322M	10.60	23.60	52.60	3.63	14.90	38.60
	NCI-H460	4.27	24.00	> 100	4.44	16.90	49.00
	NCI-H522	10.40	22.80	50.10	4.46	18.00	42.90
Colon Cancer							
	COLO 205	13.00	30.80	73.40	11.60	26.70	61.30
	HCC-2998	23.50	51.90	> 100	16.60	34.50	71.50
	HCT-116	4.09	21.00	> 100	3.77	14.30	37.80
	HCT-15	6.88	66.30	> 100	5.48	22.40	71.10
	HT29	5.66	24.20	> 100	6.39	19.20	47.00
	KM12	7.34	23.90	67.90	9.34	21.20	46.10
	SW-620	6.48	36.00	> 100	5.60	19.10	52.80
CNS Cancer							
	SF-268	5.60	29.20	> 100	5.56	21.00	58.70
	SF-295	13.30	40.10	> 100	–	–	–
	SF-539	14.60	55.90	> 100	15.30	28.90	54.40
	SNB-19	14.20	40.80	> 100	14.40	31.80	70.20
	SNB-75	12.20	25.00	51.60	13.60	26.50	51.50
	U251	13.30	28.00	59.00	7.40	20.60	46.00
Melanoma							
	LOX IMVI	1.97	4.10	8.54	1.87	3.75	7.55
	MALME-3 M	7.97	26.30	78.50	8.38	22.50	53.60
	M14	7.03	40.90	> 100	11.10	26.50	63.40
	MDA-MB-435	4.02	23.10	> 100	7.10	26.90	84.50
	SK-MEL-2	3.15	9.08	59.20	–	–	–
	SK-MEL-28	12.70	29.60	68.70	15.30	29.80	57.90
	SK-MEL-5	3.92	14.80	40.50	4.74	16.90	43.10
	UACC-257	10.6	33.60	> 100	7.15	22.20	55.30
	UACC-62	5.18	19.50	49.90	–	–	–
Ovarian Cancer							
	IGROV1	5.29	22.90	99.20	2.23	5.41	22.10
	OVCAR-3	9.70	24.80	62.40	13.70	26.60	51.60
	OVCAR-4	–	–	–	15.10	30.50	61.60
	OVCAR-5	17.40	79.30	> 100	15.40	29.80	58.00
	OVCAR-8	8.10	41.70	> 100	8.07	31.50	> 100
	NCI/ADR-RES	18.80	77.40	> 100	14.70	44.70	> 100
	SK-OV-3	22.00	> 100	> 100	15.40	44.30	> 100
Renal Cancer							
	786-0	4.64	19.70	73.00	10.80	23.10	49.60
	A498	15.50	29.50	56.20	14.20	27.20	52.20
	ACHN	4.24	17.40	63.30	6.32	20.80	53.90
	CAKI-1	3.22	11.70	44.40	2.45	6.42	24.20
	RXF 393	3.18	9.98	39.90	3.77	18.10	72.70
	SN12C	3.56	17.10	83.00	3.69	18.10	70.30
	TK-10	7.13	25.00	77.10	6.81	20.70	50.50
	UO-31	3.81	15.50	44.80	4.49	17.60	43.60
Prostate Cancer							
	PC-3	13.40	31.90	76.20	16.20	30.30	56.70
	DU-145	11.50	25.60	56.70	14.30	27.30	52.30
Breast Cancer							
	MCF7	2.85	24.60	> 100	3.10	16.10	54.20
	MDA-MB-231/ATCC	5.27	24.20	95.40	9.39	25.60	67.10
	HS 578T	18.30	53.90	> 100	18.10	58.30	> 100
	BT-549	2.59	8.33	98.20	1.90	3.83	7.73
	T-47D	4.30	22.30	98.20	4.69	20.30	68.60
	MDA-MB-468	1.96	4.59	25.20	1.98	7.32	76.80

Table 3
Median growth inhibitory concentrations[a] (GI_{50}, μM) of *in vitro* subpanel tumour cell lines.

Subpanel cell line	Compound			
	2f		4a	
	MG-MID	Selectivity index	MG-MID	Selectivity index
Leukemia	12.82	0.74	6.66	1.31
Non-small cell lung cancer	12.14	0.78	8.74	0.99
Colon cancer	9.56	0.99	8.39	1.04
CNS cancer	12.20	0.78	11.25	0.77
Melanoma	6.28	1.51	7.95	1.09
Ovarian cancer	13.55	0.70	12.09	0.72
Renal cancer	5.66	1.68	6.57	1.32
Prostate cancer	12.45	0.76	15.25	0.57
Breast cancer	5.88	1.62	6.53	1.33
Full panel MG-MID[b]	9.51		8.69	

[a] Median value calculated according to the data obtained from NCI's *in vitro* disease-oriented human tumour cell screen.
[b] GI_{50} (μM) full panel mean-graph mid point(MG-MID) = the average sensitivity of all cell lines towards the test agents.

Table 4
Median total growth inhibitory concentrations[a] (TGI, μM) of *in vitro* subpanel tumor cell lines.

Subpanel cell line	Compound			
	2f		4a	
	MG-MID	Selectivity index	MG-MID	Selectivity index
Leukemia	> 100	0.30	29.97	0.82
Non-small cell lung cancer	36.56	0.82	26.17	0.94
Colon cancer	36.30	0.83	22.49	1.09
CNS cancer	36.50	0.83	25.76	0.95
Melanoma	22.33	1.35	21.22	1.16
Ovarian cancer	57.68	0.52	30.40	0.81
Renal cancer	18.24	1.65	19.00	1.29
Prostate cancer	28.75	1.05	28.80	0.85
Breast cancer	22.99	1.30	21.91	1.12
Full panel MG-MID[b]	30.13		24.53	

[a] Median value calculated according to the data obtained from NCI's *in vitro* disease-oriented human tumor cell screen.
[b] TGI (μM) full panel mean-graph mid point(MG-MID) = the average sensitivity of all cell lines toward the test agents.

quinolone moieties that is connected to the triazolopyridazine through a spacer, which is absent in our compounds (Fig. 4, bottom). The docking score of the compounds showing the highest activity are listed in Table 6.

Table 5
Inhibition activity of **2f** and **4a** towards c-Met kinase receptor.

Compound	% c-Met kinase activity Concentration (μM)							IC_{50} (μM)
	0.001	0.01	0.1	1	10	50	100	
2f	−3	−3	−5	−9	−17	−38	−51	106.9
4a	−1	1	0	−5	−8	−22	−35	242.2

The intra-assay variability is less than 10%.
Only values of more than 25% change in activity compared to the control are considered to be significant.

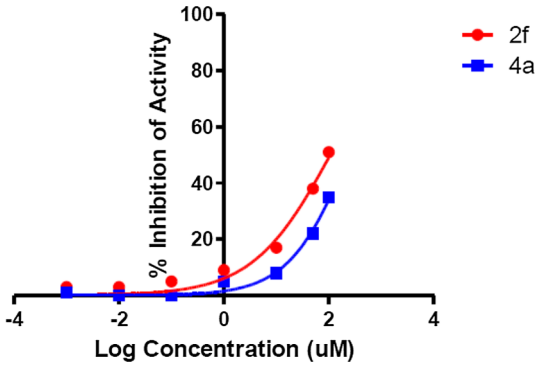

Fig. 2. Dose response curve for compounds **2f** and **4a** (log inhibitor concentration (μM) *vs.* % normalized c-Met kinase activity).

2.4. Structure activity relationship

Upon examination of both the biological screening results, as well as the docking results it was found that the use of an oxygen spacer, instead of carbon between the pyradizine ring and substituted aromatic ring resulted in a compound that showed poor activity (**4b**). Additionally, the substituted of the aromatic ring attached to the pyridazine with a heterocyclic ring produced a compound with no cytotoxic activity (**6a** & **6b**). Similarly, the substitution of the aromatic ring with a sulphonamide or a carbamimidoylsulphonamide group yielded compounds with little or no cytotoxic activity (**2e**). The use of halogen substituents yielded mixed results, monohalogenated compounds produced compounds with moderate activity (**2a**, **2b**, **2c** & **2i**), while the dihalogenated derivative showed poor activity (**2d**). Similarly, the use of carboxylic acid substituent also yielded mixed results, the addition of the carboxylic acid substituent in position 3 or 4 produced compounds that showed little or no activity (**2g** & **2h**), while the addition of the carboxylic acid group position 2 produced a compound that showed excellent cytotoxic activity (**2f**). The compound bearing an amide substitution at position 2 of the phenyl ring showed the highest cytotoxic activity (**4a**).

3. Experimental

3.1. Chemical synthesis

All chemicals and reagents were obtained from Aldrich (Sigma–Aldrich, St. Louis, MO, USA), and were used without further purification. Reactions were monitored by TLC, performed on silica gel glass plates containing 60 GF-254, and visualization on TLC was achieved by UV light or iodine indicator. IR spectra were determined on Shimadzu IR 435 spectrophotometer (KBr, cm^{-1}). ^1H NMR spectra were carried out using a Mercury 300-BB 300 MHz using TMS as an internal standard. Chemical shifts (δ) were recorded in ppm on δ scale, Micro analytical Centre, Cairo University, Egypt. ^{13}C NMR spectra were carried out using a Mercury 300-BB 75 MHz using TMS as an internal standard. Chemical shifts (δ) were recorded in ppm on δ scale, Micro analytical Centre, Cairo University, Egypt. Mass spectra were recorded on Shimadzu Qp-2010 plus Spectrometer, Micro analytical Centre, Cairo University, Egypt. Elemental analyses were carried out at the Micro analytical Centre, Cairo University, Egypt. Their results corresponded to the calculated values within ± 0.4% experimental error. Melting points were determined with Stuart apparatus and are uncorrected.

The starting material, 3,6-dichloropyridazine was commercially available. The key intermediates; 6-chloro-3-substituted-aminopyridazines [21,22] **1a-e** and **1 g,h** 2-(6-chloropyridazine-3-yloxy)benzamide [21] **(3b)** 4-(6-chloropyridazin-3-ylamino)benzene sulphonamide [22] (**5a**) and *N*-carbamimidoyl-4-[(6-chloropyridazin-3-yl)amino] benzene sulphonamide [22] **(5b)** were prepared according to the reported procedures.

3.1.1. General procedure for *1f, 1i and 3a*

A mixture of 3,6-dichloropyridazine (1.48 g, 0.01 mol), anhydrous K_2CO_3 (0.02 mol) and the appropriate amino compound (0.01 mol) in isopropanol (30 mL) was heated under reflux for 4–5 h. The reaction mixture was concentrated under reduced pressure to half its volume and cooled. The separated solid was filtered, washed with water (20 mL), dried and crystallized from isopropanol.

3.1.2. 2-(6-Chloropyridazin-3-ylamino)benzoic acid *(1f)*

Yield 72%; mp 220–221 °C; IR (KBr) (cm^{-1}): 3400–2318 (br., O—H and N—H), 1747 (C═O), 1620 (C═N); ^1H NMR (300 MHz, DMSO-d_6) δ: 7.60–7.65 (m, 2H, Ar-H), 7.69 (d, 1H, pyridazine, J = 9.9 Hz), 7.80 (d, 1H, Ar-H, J = 8.7 Hz), 7.94 (d, 1H, pyridazine, J = 9.9 Hz), 8.32 (d, 1H, Ar-H, J = 8.7 Hz); MS (EI, 70 ev) m/z (%): 249 (M^+, 0.1), 205 (3.2), 137 (0.8), 128 (1.3), 121 (0.9), 113 (5.3). Anal. Calcd for $C_{11}H_8ClN_3O_2$

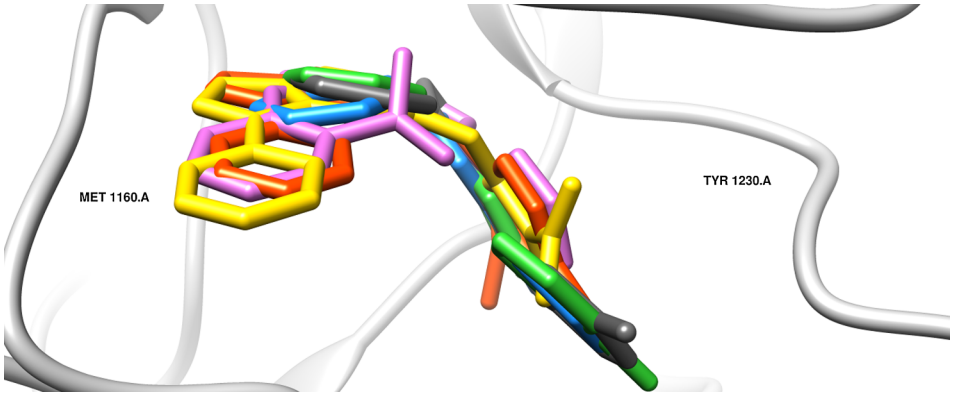

Fig. 3. Orientation of compounds 2a (green), 2b (blue), 2c (grey), 2f (pink), 2i (orange) & 4a (yellow) in the ATP binding site of c-Met kinase. Hydrogen atoms not shown for clarity.

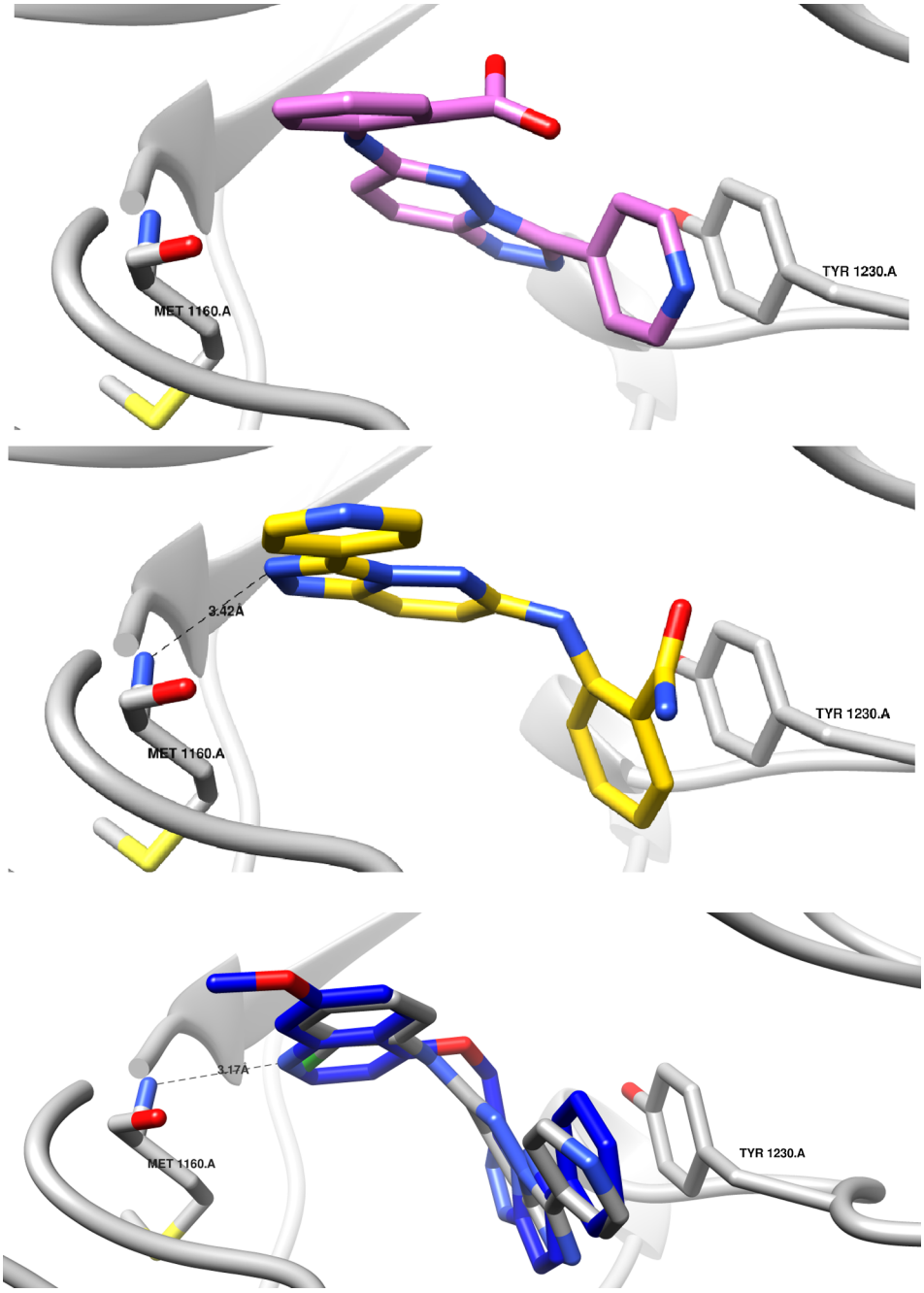

Fig. 4. Binding modes of compounds 2f, shown in purple (top), 4a, shown in yellow (middle), compound 2c, shown in grey, superimposed with the crystal structure of ligand I, shown in blue (bottom), in the c-Met kinase binding pocket. Images showing key interacting residues, as well as key interactions formed. Hydrogen atoms not shown for clarity.

(249.65): C, 52.92; H, 3.23; N, 16.83, Found, C, 52.66; H, 2.94; N, 16.95.

3.1.3. 5-Chloro-2-(6-chloropyridazin-3-ylamino)benzoic acid ***(1i)***

Yield 70%; mp 204–205 °C; IR (KBr) (cm^{-1}): 3433–2364 (br., O—H and N—H), 1728 (C=O), 1616 (C=N); ^{1}H NMR (300 MHz, DMSO-d_6) δ: 7.62–7.65 (m, 2H, Ar-H), 7.70 (d, 1H, pyridazine, J = 9.9 Hz), 7.87 (s, 1H, NH, D_2O exchangeable), 7.95 (d, 1H, pyridazine, J = 9.9 Hz), 8.30 (s, 1H, Ar-H); MS (EI, 70 ev) m/z (%): 283 (M^+, 0.05), 239 (5.6), 171 (0.2), 128 (0.4), 113 (1.7). Anal. Calcd for $C_{11}H_7Cl_2N_3O_2$ (284.10): C,

Table 6
Docking score and interactions of the compounds showing the highest activity (**2f & 4a**).

Compound	Energy score (Kcal/mol)	Amino acid	Interacting group	Length (Å)
2f	−7.53	Tyr 1230 (π-π stacking)	Pyrimidine ring	3.75
4a	−6.88	Tyr 1230 (π-π stacking)	Phenyl ring	3.65
		Met 1160 (H-bond)	N of triazole ring	3.20

46.50; H, 2.48; N, 14.79, Found, C, 46.30; H, 2.65; N, 14.98.

*3.1.4. 2-(6-Chloropyridazin-3-ylamino)benzamide **(3a)***

Yield 68%; mp 150–151 °C; IR (KBr) (cm^{-1}): 3401, 3392 (NH_2), 3350 (N−H), 1710 (C═O), 1619 (C═N); ^{1}H NMR (300 MHz, DMSO-d_6) δ: 7.36 (s, 2H, NH_2, D_2O exchangeable), 7.61 (d, 1H, pyridazine, J = 9.6 Hz), 7.77–7.92 (m, 3H, Ar-H), 7.95 (d, 1H, pyridazine, J = 9.6 Hz), 8.30 (d, 1H, Ar-H, J = 9.3 Hz); MS (EI, 70 ev) m/z (%): 250 (M + 2, 14.87), 248 (M^+, 15.6), 231 (100.0), 135 (0.7), 113 (24.5). Anal. Calcd for $C_{11}H_9ClN_4O$ (248.67): C, 53.13; H, 3.65; N, 22.53, Found, C, 52.95; H, 3.74; N, 22.48.

*3.1.5. General procedure **2a-i, 4a,b** and **6a,b***

A solution of an appropriate either of **1a-i** or **3a,b** or **5a,b** (0.001 mol) and isonicotinic acid hydrazide (0.14 g, 0.001 mol) in n-butanol (20 mL) was heated under reflux for 6–8 h. The solution was filtered while hot, the filtrate was concentrated under reduced pressure to half its volume and cooled. The separated solid was filtered, washed by sodium carbonate solution (10%, 20 mL), then crystallized from benzene.

*3.1.6. N-(2-Bromophenyl)-3-(pyridin-4-yl)-[1,2,4]triazolo[4,3-b] pyridazin-6-amine **(2a)***

Yield 76%; mp 220–221 °C; IR (KBr) (cm^{-1}): 3383 (N−H), 1631 (C═N); ^{1}H NMR (300 MHz, DMSO-d_6) δ: 7.63 (d, 1H, pyridazine, J = 9.9 Hz), 7.84–7.92 (m, 2H, Ar-H), 8.40–8.45 (m, 2H, Ar-H), 8.52 (d, 1H, pyridazine, J = 9.9 Hz), 8.80 (d, 2H, pyridine, J = 6.3 Hz), 8.88 (d, 2H, pyridine, J = 6.3 Hz), 10.02 (s, 1H, NH, D_2O exchangeable); MS (EI, 70 ev) m/z (%): 366 (M^+, 30.2), 288 (15.4), 197 (6.0), 92 (28.8), 91 (6.0). Anal. Calcd for $C_{16}H_{11}BrN_6$ (367.20): C, 52.33; H, 3.02; N, 22.89, Found, C, 52.56; H, 2.96; N, 22.95.

*3.1.7. N-(2-Chlorophenyl)-3-(pyridin-4-yl)-[1,2,4]triazolo[4,3-b] pyridazin-6-amine **(2b)***

Yield 65%; mp 209–210 °C; IR (KBr) (cm^{-1}): 3417 (N−H), 1631 (C═N); ^{1}H NMR (300 MHz, DMSO-d_6) δ: 7.51–7.61 (m, 2H, Ar-H), 7.77 (d, 1H, pyridazine, J = 9.6 Hz), 8.14–8.17 (m, 2H, Ar-H), 8.38 (d, 1H, pyridazine, J = 9.6 Hz), 8.95 (d, 2H, pyridine, J = 6 Hz), 8.99 (d, 2H, pyridine, J = 6 Hz), 9.86 (s, 1H, NH, D_2O exchangeable); MS (EI, 70 ev) m/z (%): 324 (M + 2, 33.9), 322 (M^+, 100.0), 212 (4.4), 196 (31.5), 128 (16.2), 126 (4.4), 111 (22.7). Anal. Calcd for $C_{16}H_{11}ClN_6$ (322.07): C, 59.54; H, 3.44; N, 26.04, Found, C, 59.88; H, 3.56; N, 26.14.

*3.1.8. N-(4-Chlorophenyl)-3-(pyridin-4-yl)-[1,2,4]triazolo[4,3-b] pyridazin-6-amine **(2c)***

Yield 68%; mp 275–276 °C; IR (KBr) (cm^{-1}): 3267 (N−H), 1635 (C═N); ^{1}H NMR (300 MHz, DMSO-d_6) δ: 7.27 (d, 1H, pyridazine, J = 9 Hz), 7.48 (d, 2H, Ar-H, J = 8.4 Hz), 7.70 (d, 2H, Ar-H, J = 8.4 Hz), 8.20 (d, 1H, pyridazine, J = 9 Hz), 8.52 (d, 2H, pyridine, J = 6.3 Hz), 8.98 (d, 2H, pyridine, J = 6.3 Hz), 10.39 (s, 1H, NH, D_2O exchangeable); ^{13}C NMR (DMSO-d_6 ppm) δ: 118.6, 120.7, 121.3, 121.6, 126.4, 128.7, 137.3, 138.0, 143.5, 144.5, 146.3, 149.7 (aromatic C's); MS (EI, 70 ev) m/z (%): 324 (M + 2, 33.6), 322 (M^+, 100.0), 212 (7.9), 196 (48.5), 126 (8.3), 111 (43.7), 91 (8.4). Anal. Calcd for $C_{16}H_{11}ClN_6$ (322.07): C, 59.54; H, 3.44; N, 26.04, Found, C, 59.46; H, 3.48; N, 25.88.

*3.1.9. N-(2,6-Dichlorophenyl)-3-(pyridin-4-yl)-[1,2,4]triazolo[4,3-b] pyridazin-6-amine **(2d)***

Yield 84%; mp 245–246 °C; IR (KBr) (cm^{-1}): 3394 (N−H), 1631 (C═N); ^{1}H NMR (300 MHz, DMSO-d_6) δ: 7.64 (d, 1H, pyridazine, J = 9.6 Hz), 7.84–7.93 (m, 1H, Ar-H), 8.35 (d, 1H, pyridazine, J = 9.6 Hz), 8.60 (d, 2H, Ar-H, J = 9.6 Hz), 8.80 (d, 2H, pyridine, J = 6 Hz), 8.88 (d, 2H, pyridine, J = 6 Hz), 10.02 (s, 1H, NH, D_2O exchangeable); MS (EI, 70 ev) m/z (%): 360 (M + 4, 0.4), 358 (M + 2, 0.4), 211 (1.9), 196 (2.0), 161 (3.2), 145 (2.9). Anal. Calcd for $C_{16}H_{10}Cl_2N_6$ (357.20): C, 53.80; H, 2.82; N, 23.50, Found, C, 53.70; H, 2.45; N, 23.23.

*3.1.10. N-(2-Chloropyridin-3-yl)-3-(pyridin-4-yl)-[1,2,4]triazolo[4,3-b] pyridazin-6-amine **(2e)***

Yield 70%; mp 269–270 °C; IR (KBr) (cm^{-1}): 3394 (N−H), 1631 (C═N); ^{1}H NMR (300 MHz, DMSO-d_6) δ: 7.68 (d, 1H, pyridazine, J = 9.6 Hz), 7.92–8.51 (m, 3H, pyridine), 8.64 (d, 1H, pyridazine, J = 9.6 Hz), 8.84 (d, 2H, pyridine, J = 6.3 Hz), 8.94 (d, 2H, pyridine, J = 6.3 Hz), 10.19 (s, 1H, NH, D_2O exchangeable); MS (EI, 70 ev) m/z (%): 325 (M + 2, 1.4), 323 (M^+, 0.1), 211 (0.6), 196 (100.0), 146 (1.9), 127 (1.1), 92 (9.1). Anal. Calcd for $C_{15}H_{10}ClN_7$ (323.74): C, 55.65; H, 3.11; N, 30.29, Found, C, 55.76; H, 2.95; N, 30.45.

*3.1.11. 2-[3-(Pyridin-4-yl)-[1,2,4]triazolo[4,3-b]pyridazin-6-ylamino] benzoic acid **(2f)***

Yield 72%; mp 200–201 °C; IR (KBr) (cm^{-1}): 3390–2476 (br., O−H), 3244 (N−H), 1708 (C═O), 1624 (C═N); ^{1}H NMR (300 MHz, DMSO-d_6) δ: 7.58–7.79 (m, 3H, Ar-H), 7.91 (d, 1H, pyridazine, J = 9.3 Hz), 7.94–7.97 (m, 1H, Ar-H), 8.32 (d, 1H, pyridazine, J = 9.3 Hz), 8.64 (d, 2H, pyridine, J = 6 Hz), 8.80 (d, 2H, pyridine, J = 6 Hz), 10.21 (s, 1H, NH, D_2O exchangeable); ^{13}C NMR (DMSO-d_6 ppm) δ: 119.0, 119.1, 126.7, 126.8, 126.9, 127.1, 127.2, 128.7, 135.1, 135.2, 137.5, 144.2, 146.6, 146.7 (aromatic C's), 156.7 (C═O); MS (EI, 70 ev) m/z (%): 332 (M^+, 2.3), 211 (0.9), 121 (6.5), 136 (1.7), 93 (11.1). Anal. Calcd for $C_{17}H_{12}N_6O_2$ (332.32): C, 61.44; H, 3.64; N, 25.29, Found, C, 61.76; H, 3.23; N, 25.43.

*3.1.12. 3-[3-(Pyridin-4-yl)-[1,2,4]triazolo[4,3-b]pyridazin-6-ylamino] benzoic acid **(2g)***

Yield 76%; mp > 300 °C; IR (KBr) (cm^{-1}): 3400–2538 (br., O−H), 3290 (N−H), 1685 (C═O), 1631 (C═N); ^{1}H NMR (300 MHz, DMSO-d_6) δ: 7.25 (d, 1H, pyridazine, J = 9.9 Hz), 7.50–7.73 (m, 3H, Ar-H), 8.24 (d, 1H, pyridazine, J = 9.9 Hz), 8.50 (d, 2H, pyridine, J = 6 Hz), 8.63 (s, 1H, Ar-H), 8.84 (d, 2H, pyridine, J = 6 Hz), 10.21 (s, 1H, NH, D_2O exchangeable), 13.00 (br, 1H, OH, D_2O exchangeable); MS (EI, 70 ev) m/z (%): 332 (M^+, 6.9), 288 (99.7), 196 (15.0), 136 (6.1), 93 (9.0). Anal. Calcd for $C_{17}H_{12}N_6O_2$ (332.32): C, 61.44; H, 3.64; N, 25.29, Found, C, 61.28; H, 3.44; N, 25.05.

*3.1.13. 4-[3-(Pyridin-4-yl)-[1,2,4]triazolo[4,3-b]pyridazin-6-ylamino] benzoic acid **(2h)***

Yield 70%; mp 240–241 °C; IR (KBr) (cm^{-1}): 3440–2546 (br., O−H), 3294 (N−H), 1666 (C═O), 1612 (C═N); ^{1}H NMR (300 MHz, DMSO-d_6) δ: 7.24 (d, 1H, pyridazine, J = 9.9 Hz), 7.30 (d, 2H, Ar-H, J = 9.3 Hz), 7.63 (d, 2H, Ar-H, J = 9.3 Hz), 8.27 (d, 1H, pyridazine, J = 9.9 Hz), 8.40 (d, 2H, pyridine, J = 6 Hz), 8.91 (d, 2H, pyridine, J = 6 Hz), 10.25 (s, 1H, NH, D_2O exchangeable), 12.55 (br, 1H, OH, D_2O exchangeable); MS (EI, 70 ev) m/z (%): 332 (M^+, 0.3), 288 (0.2), 212 (0.6), 196 (2.0), 136 (6.3), 93 (11.4). Anal. Calcd for $C_{17}H_{12}N_6O_2$ (332.32): C, 61.44; H, 3.64; N, 25.29, Found, C, 61.58; H, 3.55; N, 25.22.

*3.1.14. 5-Chloro-2-[3-(pyridin-4-yl)-[1,2,4]triazolo[4,3-b]pyridazin-6-ylamino]benzoic acid **(2i)***

Yield 62%; mp 250–251 °C; IR (KBr) (cm^{-1}): 3410–2623 (br., O−H), 3272 (N−H), 1693 (C═O), 1620 (C═N); ^{1}H NMR (300 MHz, DMSO-d_6) δ: 7.44 (d, 1H, pyridazine, J = 9.9 Hz), 7.51–7.80 (m, 2H, Ar-H), 8.01 (s, 1H, Ar-H), 8.16 (d, 1H, pyridazine, J = 9.9 Hz), 8.85 (d, 2H, pyridine, J = 6.3 Hz), 8.90 (d, 2H, pyridine, J = 6.3 Hz), 9.80 (s, 1H, NH, D_2O exchangeable), 11.13 (s, 1H, OH, D_2O exchangeable); MS (EI, 70 ev) m/z (%): 368 (M + 2, 2.9), 366 (M^+, 7.8), 321 (0.3), 212 (2.6), 196 (1.9), 169 (1.9), 125 (1.8). Anal. Calcd for $C_{17}H_{11}ClN_6O_2$ (366.76): C, 55.67; H, 3.02; N, 22.91, Found, C, 55.86; H, 2.96; N, 22.82.

*3.1.15. 2-[3-(Pyridin-4-yl)-[1,2,4]triazolo[4,3-b]pyridazin-6-ylamino] benzamide **(4a)***

Yield 75%; mp 205–206 °C; IR (KBr) (cm^{-1}): 3437, 3417 (NH_2), 3387 (N—H), 1665 (C═O), 1624 (C═N); ^1H NMR (300 MHz, DMSO-d_6) δ: 4.62 (br, 2H, NH_2, D_2O exchangeable), 6.85–6.88 (m, 3H, Ar-H), 6.98 (d, 1H, pyridazine, J = 9.9 Hz), 7.51 (d, 1H, pyridazine, J = 9.9 Hz), 7.73 (d, 1H, Ar-H, J = 6 Hz), 7.82 (d, 2H, pyridine, J = 6.3 Hz), 8.65 (s, 1H, NH, D_2O exchangeable), 8.70 (d, 2H, pyridine, J = 6.3 Hz); MS (EI, 70 ev) m/z (%): 331 (M^+, 6.2), 315 (1.9), 287 (4.1), 212 (1.3), 196 (4.6), 136 (10.8), 121 (10.8). Anal. Calcd for $C_{17}H_{13}N_7O$ (331.33): C, 61.62; H, 3.95; N, 29.59, Found, C, 61.58; H, 4.10; N, 29.65.

*3.1.16. 2-[3-(Pyridin-4-yl)-[1,2,4]triazolo[4,3-b]pyridazin-6-yloxy] benzamide **(4b)***

Yield 80%; mp 79–80 °C; IR (KBr) (cm^{-1}): 3410, 3390 (NH_2), 1666 (C═O), 1631 (C═N); ^1H NMR (300 MHz, DMSO-d_6) δ: 4.98 (br, 2H, NH_2, D_2O exchangeable), 7.60 (d, 1H, pyridazine, J = 9.9 Hz), 7.65–7.95 (m, 4H, Ar-H), 7.94 (d, 2H, pyridine, J = 6.6 Hz), 7.96 (d, 1H, pyridazine, J = 9.9 Hz), 8.35 (d, 2H, pyridine, J = 6.6 Hz); MS (EI, 70 ev) m/z (%): 332 (M^+, 0.1), 288 (0.2), 212 (0.2), 196 (0.4), 136 (0.9), 78 (87.2). Anal. Calcd for $C_{17}H_{12}N_6O_2$ (332.32): C, 61.44; H, 3.64; N, 25.29, Found, C, 61.50; H, 3.74; N, 25.43.

*3.1.17. 4-[3-(Pyridin-4-yl)-[1,2,4]triazolo[4,3-b]pyridazin-6-ylamino] benzene- sulfonamide **(6a)***

Yield 76%; mp 100–101 °C; IR (KBr) (cm^{-1}): 3464, 3356 (NH_2), 3271 (N—H), 1666 (C═O), 1631 (C═N), 1315, 1153 (SO_2); ^1H NMR (300 MHz, DMSO-d_6) δ: 5.75 (br, 2H, NH_2, D_2O exchangeable), 6.57 (d, 1H, pyridazine, J = 9.6 Hz), 6.59–7.43 (m, 4H, Ar-H), 6.85 (s, 1H, NH, D_2O exchangeable), 7.45 (d, 1H, pyridazine, J = 9.6 Hz), 7.73 (d, 2H, pyridine, J = 6 Hz), 8.70 (d, 2H, pyridine, J = 6 Hz); MS (EI, 70 ev) m/z (%): 368 (M + H, 13.6), 367 (M^+, 15.5), 352 (18.6), 287 (13.6), 78 (85.0). Anal. Calcd for $C_{16}H_{13}N_7O_2S$ (367.39): C, 52.31; H, 3.57; N, 26.69, Found, C, 52.16; H, 3.66; N, 26.73.

*3.1.18. N-Carbamimidoyl-4-[3-(pyridin-4-yl)-[1,2,4]triazolo[4,3-b] pyridazin-6-ylamino] benzenesulfonamide **(6b)***

Yield 72%; mp 129–130 °C; IR (KBr) (cm^{-1}): 3417, 3325 (NH_2), 3201 (N—H), 1631 (C═N), 1323, 1134 (SO_2); ^1H NMR (300 MHz, DMSO-d_6) δ: 4.41 (br, 2H, NH_2, D_2O exchangeable), 6.63 (d, 2H, Ar-H, J = 8.7 Hz), 6.75 (s, 1H, NH, D_2O exchangeable), 7.43 (d, 2H, Ar-H, J = 8.7 Hz), 7.68 (d, 1H, pyridazine, J = 9.3 Hz), 8.43 (d, 2H, pyridine, J = 6.3 Hz), 8.64 (d, 1H, pyridazine, J = 9.3 Hz), 8.91 (d, 2H, pyridine, J = 6.3 Hz), 10.00 (s, 1H, NH, D_2O exchangeable), 11.02 (s, 1H, NH, D_2O exchangeable); MS (EI, 70 ev) m/z (%): 409 (M^+, 0.1), 393 (0.1), 351 (0.2), 287 (0.3), 213 (4.9), 196 (8.9), 123 (13.2), 78 (4.4) 57 (100.0). Anal. Calcd for $C_{17}H_{15}N_9O_2S$ (409.43): C, 49.87; H, 3.69; N, 30.79; Found, C, 49.96; H, 3.45; N, 30.88.

3.2. Biological studies

3.2.1. Cytotoxic activity

The cytotoxic activity of the synthesized target compounds (**2a-i**, **4a, b** and **6a, b**) was evaluated using the NCI's disease-oriented human cell lines screening assay. The cytotoxic assays were performed in accordance with the protocol of the Drug Evaluation Branch, NCI, Bethesda, MD, USA. Initially, all the synthesized compounds were first evaluated at a single concentration of 10^{-5} M towards a panel of approximately 60 cancer lines. The human tumor cell lines used were derived from nine different cancer types: leukemia, melanoma, lung, colon, CNS, ovarian, renal, prostate and breast cancers. The cultures were incubated for 48 h, and the sulforhodamine B (SRB) protein assay was employed as previously reported [28–31]. Compounds showing significant cytotoxic activity, were then reevaluated using 5 different concentrations ranging for 10^{-4}–10^{-8} M. To estimate the cell viability and growth; a 48 h drug exposure protocol and sulforhodamine B (SRB) protein assay were employed [28–31]. The results were reported as the percentage growth of the treated cells in comparison to the untreated control cells. Additionally, a dose response curve was plotted and the following parameters, GI_{50}, representing the molar concentration of the tested compound that results in a 50% decrease in cell growth, TGI, representing the molar concentration of the tested compound that results in total growth inhibition and LC_{50}, reflecting the molar concentration of the tested compound that results in 50% net cell death were calculated.

3.2.2. In vitro c-Met kinase inhibition

Using proprietary methods; c-Met kinase was cloned, expressed and purified to be employed in the compound profiling process. Moreover, quality control testing was regularly done to ensure compliance to acceptable standards. ^{33}P-ATP was purchased from PerkinElmer, while all other materials were of standard laboratory grade. Stock solution of the synthesized compounds was prepared in DMSO, which was then diluted to be used for profiling against c-Met protein kinase.

To evaluate the profiling of the protein kinase target; a radioisotope assay format was employed and all assays were performed in a designated radioactive working area. Protein kinase assays were performed in singlicates at room temperature for 20–30 min in a final volume of 25 µl according to the following assay reaction recipe: Component 1. 5 µl of diluted active c-Met (~10–50 nM final concentration in the assay), component 2.5 µl of stock solution of substrate, component 3.5 µl of kinase assay buffer, component 4.5 µl of compound (various concentration) or 10% DMSO and component 5.5 µl of ^{33}P-ATP (250 µM stock solution, 0.8 µCi).

^{33}P-ATP was added to initiate the assay and the reaction mixture was incubated at room temperature for 20–30 min. To terminate the assay after the incubation period; 10 µl of the reaction mixture were spotted onto multiscreen phosphocellulose P81 plate, which was then washed 3 times in 1% phosphoric acid solution for approximately 15 min. The radioactivity on the P81 plate was counted using a Trilux scintillation counter in the presence of scintillation fluid. A blank control was set up in the same manner, however, the appropriate substrate was replaced with equal volume of assay dilution buffer. Finally, to determine the corrected activity for protein kinase target; the blank control values were removed [24,25].

3.3. Molecular docking

Molecular docking in the ATP binding site of c-Met was carried out for all the synthesized compounds using Autodock 4.2 [32]. The crystal structure of c-Met kinase (PDB code: 3CD8) [15] was downloaded from the protein databank (https://www.rcsb.org/pdb) [33] and was prepared using Autodock tools [32]. All water molecules were deleted from the crystal structure before docking. This was then followed by assigning partial charges using Gasteiger charges to both the protein structure and ligands. The binding pocket was defined using a grid box cantered on the native ligand with dimensions 60 × 60 × 60 points with a spacing of 0.375 Å. The Lamarckian genetic algorithm was used to carry out a 100 docking runs for each compound using the default Autodock parameters [32]. UCSF Chimera [34] was then used to visualize and analyse the results.

4. Conclusion

This study reports the synthesis and anticancer activity assessment of 3-(pyridin-4-yl)-**[1,2,4]** triazolo[4,3-*b*]pyridazine derivatives **2a-i**, **4a,b** and **6a,b** according to the protocol of the Drug Evaluation Branch, NCI, USA**.** Interestingly, the majority of the tested compounds demonstrated promising activity against various leukaemia cell panels. Two compounds, namely **2f** and **4a,** bearing carboxylic acid and carboxamide substituents respectively at the 2- position of the phenyl ring

scaffold, emerged as promising cytotoxic agents against the entire panel of tumor cell lines. The MG-MID GI_{50} (μM) values of the two most potent analogs **2f** and **4a** recorded 9.51 and 8.69 respectively. Additionally, these compounds also showed significant activity as c-Met kinase inhibitors, with IC_{50} values of 106.9 μM and 242.2 μM, respectively.

The docking results of compound **4a** showed a different binding orientation to that previously reported for triazolopyrridazine derivatives. The further derivatization of this compound, should allow the exploitation the chance for formation of another hydrogen bond with the backbone of Asp1222 residue of the C-met kinase receptor. This additional hydrogen bond is reported to increase the selectivity and potency towards the C-met kinase and thus the cytotoxic activity. Therefore, it is likely that the further derivatization of this could will be of interest in the hope of yielding more selective anticancer agents.

Declaration of Competing Interest

The authors declare that they have no known competing financial interests or personal relationships that could have appeared to influence the work reported in this paper.

Acknowledgment

Thanks are due to the NCI, Bethesda, MD, U.S.A. for performing the antitumor testing of the synthesized compounds and for Kinexus, Canada for performing the c-Met inhibition activity.

References

[1] X. Liu, W. Yao, R.C. Newton, P.A. Scherle, Targeting the c-MET signaling pathway for cancer therapy, Exp. Opin. Invest. Drugs 17 (7) (2008) 997–1011.
[2] C. Schmidt, F. Bladt, S. Goedecke, V. Brinkmann, W. Zschiesche, M. Sharpe, E. Gherardi, C. Birchmeler, Scatter factor/hepatocyte growth factor is essential for liver development, Nature 373 (6516) (1995) 699.
[3] Y. Uehara, O. Minowa, C. Mori, K. Shiota, J. Kuno, T. Noda, N. Kitamura, Placental defect and embryonic lethality in mice lacking hepatocyte growth factor/scatter factor, Nature 373 (6516) (1995) 702.
[4] K. Kawaida, K. Matsumoto, H. Shimazu, T. Nakamura, Hepatocyte growth factor prevents acute renal failure and accelerates renal regeneration in mice, PNAS 91 (10) (1994) 4357–4361.
[5] T. Nakamura, S. Mizuno, K. Matsumoto, Y. Sawa, H. Matsuda, T. Nakamura, Myocardial protection from ischemia/reperfusion injury by endogenous and exogenous HGF, J. Clin. Investig. 106 (12) (2000) 1511–1519.
[6] H. Tsubouchi, Y. Niitani, S. Hirono, H. Nakayama, E. Gohda, N. Arakaki, O. Sakiyama, K. Takahashi, M. Kimoto, S. Kawakami, Levels of the human hepatocyte growth factor in serum of patients with various liver diseases determined by an enzyme-linked immunosorbent assay, Hepatology 13 (1) (1991) 1–5.
[7] C. Birchmeier, W. Birchmeier, E. Gherardi, G.F. Vande Woude, Met, metastasis, motility and more, Nat. Rev. Mol. Cell Biol. 4 (2003) 915.
[8] C.R. Maroun, T. Rowlands, The Met receptor tyrosine kinase: a key player in oncogenesis and drug resistance, Pharmacol. Ther. 142 (3) (2014) 316–338.
[9] P.M. Comoglio, S. Giordano, L. Trusolino, Drug development of MET inhibitors: targeting oncogene addiction and expedience, Nat. Rev. Drug Discov. 7 (2008) 504.
[10] Z.-G. Sun, Y.-A. Yang, Z.-G. Zhang, H.-L. Zhu, Optimization techniques for novel c-Met kinase inhibitors, Exp. Opin. Drug Discov. 14 (1) (2019) 59–69.
[11] S.M. Malik, V.E. Maher, K.E. Bijwaard, R.L. Becker, L. Zhang, S.W. Tang, P. Song, Q. Liu, A. Marathe, B. Gehrke, W. Helms, D. Hanner, R. Justice, R. Pazdur, U.S. Food and Drug Administration Approval: Crizotinib for treatment of advanced or metastatic non-small cell lung cancer that is anaplastic lymphoma kinase positive, Clin. Canc. Res. 20 (8) (2014) 2029–2034.
[12] L. Rimassa, E. Assenat, M. Peck-Radosavljevic, M. Pracht, V. Zagonel, P. Mathurin, E. Rota Caremoli, C. Porta, B. Daniele, L. Bolondi, V. Mazzaferro, W. Harris, N. Damjanov, D. Pastorelli, M. Reig, J. Knox, F. Negri, J. Trojan, C. López López, N. Personeni, T. Decaens, M. Dupuy, W. Sieghart, G. Abbadessa, B. Schwartz, M. Lamar, T. Goldberg, D. Shuster, A. Santoro, J. Bruix, Tivantinib for second-line treatment of MET-high, advanced hepatocellular carcinoma (METIV-HCC): a final analysis of a phase 3, randomised, placebo-controlled study, Lancet Oncol. 19 (5) (2018) 682–693.
[13] K. Traynor, Cabozantinib approved for advanced medullary thyroid cancer, Am. J. Health Syst. Pharm. 70 (2) (2013) 88.
[14] T.C.C. Yau, R. Lencioni, W. Sukeepaisarnjaroen, Y. Chao, C.-J. Yen, W. Lausoontornsiri, P.-J. Chen, T. Sanpajit, A. Camp, D.S. Cox, R.C. Gagnon, Y. Liu, K.E. Raffensperger, D.A. Kulkarni, H. Kallender, L.H. Ottesen, R.T.P. Poon, D.P. Bottaro, A phase I/II multicenter study of single-agent foretinib as first-line therapy in patients with advanced hepatocellular carcinoma, Clin. Canc. Res. Off. J. Am. Assoc. Canc. Res. 23 (10) (2017) 2405–2413.
[15] B.K. Albrecht, J.-C. Harmange, D. Bauer, L. Berry, C. Bode, A.A. Boezio, A. Chen, D. Choquette, I. Dussault, C. Fridrich, Discovery and optimization of triazolopyridazines as potent and selective inhibitors of the c-Met kinase, J. Med. Chem. 51 (10) (2008) 2879–2882.
[16] A.A. Boezio, L. Berry, B.K. Albrecht, D. Bauer, S.F. Bellon, C. Bode, A. Chen, D. Choquette, I. Dussault, S. Hirai, P. Kaplan-Lefko, J.F. Larrow, M.-H.J. Lin, J. Lohman, M.H. Potashman, K. Rex, M. Santostefano, K. Shah, R. Shimanovich, S.K. Springer, Y. Teffera, Y. Yang, Y. Zhang, J.-C. Harmange, Discovery and optimization of potent and selective triazolopyridazine series of c-Met inhibitors, Bioorg. Med. Chem. Lett. 19 (22) (2009) 6307–6312.
[17] J.W. Ryu, S.-Y. Han, J.I. Yun, S.-U. Choi, H. Jung, J.D. Ha, S.Y. Cho, C.O. Lee, N.S. Kang, J.S. Koh, H.R. Kim, J. Lee, Design and synthesis of triazolopyridazines substituted with methylisoquinolinone as selective c-Met kinase inhibitors, Bioorg. Med. Chem. Lett. 21 (23) (2011) 7185–7188.
[18] M. Sattler, R. Hasina, M.M. Reddy, T. Gangadhar, R. Salgia, The role of the c-Met pathway in lung cancer and the potential for targeted therapy, Therap. Adv. Med. Oncol. 3 (4) (2011) 171–184.
[19] T.L. Underiner, T. Herbertz, S.J. Miknyoczki, Discovery of small molecule c-Met inhibitors: evolution and profiles of clinical candidates, anti-cancer agents in medicinal, Chem.- Anti-Cancer Age. 10 (1) (2010) 7–27.
[20] S.G. Buchanan, J. Hendle, P.S. Lee, C.R. Smith, P.-Y. Bounaud, K.A. Jessen, C.M. Tang, N.H. Huser, J.D. Felce, K.J. Froning, M.C. Peterman, B.E. Aubol, S.F. Gessert, J.M. Sauder, K.D. Schwinn, M. Russell, I.A. Rooney, J. Adams, B.C. Leon, T.H. Do, J.M. Blaney, P.A. Sprengeler, D.A. Thompson, L. Smyth, L.A. Pelletier, S. Atwell, K. Holme, S.R. Wasserman, S. Emtage, S.K. Burley, S.H. Reich, SGX523 is an exquisitely selective, ATP-competitive inhibitor of the MET receptor tyrosine kinase with antitumor activity *in vivo*, Mol. Cancer Ther. 8 (12) (2009) 3181–3190.
[21] K.A.M. Abouzid, N.A. Khalil, E.M. Ahmed, A. Esmat, A.M. Al-Abd, Design, synthesis, and evaluation of anti-inflammatory and ulcerogenicity of novel pyridazinone derivatives, Med. Chem. Res. 21 (11) (2012) 3581–3590.
[22] K.A.M. Abouzid, N.A. Khalil, E.M. Ahmed, K.O. Mohamed, 3-[(6-Arylamino)pyridazinylamino]benzoic acids: design, synthesis and in vitro evaluation of anticancer activity, Arch. Pharm. Res. 36 (1) (2013) 41–50.
[23] S.A. Rostom, Synthesis and in vitro antitumor evaluation of some indeno [1, 2-c] pyrazol (in) es substituted with sulfonamide, sulfonylurea (-thiourea) pharmacophores, and some derived thiazole ring systems, Bioorg. Med. Chem. 14 (19) (2006) 6475–6485.
[24] A. Furlan, F. Colombo, A. Kover, N. Issaly, C. Tintori, L. Angeli, V. Leroux, S. Letard, M. Amat, Y. Asses, B. Maigret, P. Dubreuil, M. Botta, R. Dono, J. Bosch, O. Piccolo, D. Passarella, F. Maina, Identification of new aminoacid amides containing the imidazo[2,1-b]benzothiazol-2-ylphenyl moiety as inhibitors of tumorigenesis by oncogenic Met signaling, Eur. J. Med. Chem. 47 (2012) 239–254.
[25] J.T. Rasmussen, S.M. Petiwala, J.J. Johnson, A.M. Kohl, D.N. Syed, H. Mukhtar, I.A. Siddiqui, V.M. Adhami, α-Mangostin, a xanthone from mangosteen fruit, promotes cell cycle arrest in prostate cancer and decreases xenograft tumor growth, Carcinogenesis 33 (2) (2011) 413–419.
[26] J. Porter, Small molecule c-Met kinase inhibitors: a review of recent patents, Exp. Opin. Ther. Pat. 20 (2) (2010) 159–177.
[27] E. Gherardi, W. Birchmeier, C. Birchmeier, G.V. Woude, Targeting MET in cancer: rationale and progress, Nat. Rev. Cancer 12 (2) (2012) 89.
[28] M.R. Boyd, K.D. Paull, Some practical considerations and applications of the national cancer institute in vitro anticancer drug discovery screen, Drug Dev. Res. 34 (2) (1995) 91–109.
[29] M.R. Grever, S.A. Schepartz, B.A. Chabner, The National Cancer Institute: cancer drug discovery and development program, Semin. Oncol. 19 (6) (1992) 622–638.
[30] A. Monks, A. Vaigro-Wolff, C. Hose, D. Scudiero, H. Campbell, J. Langley, M. Gray-Goodrich, P. Cronise, D. Vistica, J. Mayo, K. Paull, M. Boyd, P. Skehan, R. Shoemaker, Feasibility of a high-flux anticancer drug screen using a diverse panel of cultured human tumor cell lines, JNCI: J. Natl. Canc. Instit. 83 (11) (1991) 757–766.
[31] P. Skehan, R. Storeng, D. Scudiero, A. Monks, J. McMahon, D. Vistica, J.T. Warren, H. Bokesch, S. Kenney, M.R. Boyd, New colorimetric cytotoxicity assay for anticancer-drug screening, JNCI: J. Natl. Cancer Instit. 82 (13) (1990) 1107–1112.
[32] G.M. Morris, R. Huey, W. Lindstrom, M.F. Sanner, R.K. Belew, D.S. Goodsell, A.J. Olson, AutoDock4 and AutoDockTools4: automated docking with selective receptor flexibility, J. Comput. Chem. 30 (16) (2009) 2785–2791.
[33] H.M. Berman, J. Westbrook, Z. Feng, G. Gilliland, T.N. Bhat, H. Weissig, I.N. Shindyalov, P.E. Bourne, The protein data bank, Nucl. Acids Res. 28 (1) (2000) 235–242.
[34] E.F. Pettersen, T.D. Goddard, C.C. Huang, G.S. Couch, D.M. Greenblatt, E.C. Meng, T.E. Ferrin, UCSF Chimera—a visualization system for exploratory research and analysis, J. Comput. Chem. 25 (13) (2004) 1605–1612.